

Supplemental Methods

CLL patient samples

CLL patients were diagnosed according to International Workshop on CLL 2018 guidelines.¹ Patients indicated as “relapsed” in Table S1 had been previously treated with chemotherapy at the time of sample collection. All other patients were treatment-naïve at the time of sample collection. CD38 status was considered “positive” at a cutoff of >7% and ZAP-70 status was considered “positive” at a cutoff of >10%.

Cell Viability Assay

Cell-kill assays for viability and synergy studies were conducted using CellTiter-Blue Cell Viability Assay (Promega). Cells were plated at a density of 1×10^6 /mL in a 96-well flat-bottom plate and treated with inhibitors in a final volume of 100uL for 24 hours prior to the addition of CellTiter-Blue reagent. Synergy was determined by combination index. The combination index method is based on that previously described,² in which a combination index value of 0.85 to 0.9 indicated slight synergism, 0.7 to 0.85 indicated moderate synergism, 0.3 to 0.7 indicated synergism, 0.1 and 0.3 indicated strong synergism, and < 0.1 indicated very strong synergism.

Ex vivo murine CLL-B cell studies

Murine B cells were isolated from homogenized splenocytes by negative selection, using magnetic separation (B-cell Isolation Kit; StemCell Technologies). To detect proliferation or B-cell receptor signaling activation, B cells were stimulated by plate-bound goat antimouse immunoglobulin M F(ab')₂ fragment (Southern Biotech) for 50 minutes, prior to fixing for flow cytometry assessment.

B-cell receptor activation in CLL cell lines

Mec2 or OSU-CLL were cultured with ACY738 for 24 hours then stimulated with plate-bound goat antihuman immunoglobulin M F(ab')₂ fragment (Southern Biotech) for 50 minutes prior to fixing for flow cytometry assessment.

Immunoblotting

Samples were analyzed by SDS-PAGE (sodium dodecyl sulfate polyacrylamide gel electrophoresis), followed by transfer to nitrocellulose membrane blocked with 5% nonfat milk and incubation with indicated antibodies. Blots were developed using LI-COR system. Cell lysis was performed with radioimmunoprecipitation assay buffer (10 mM Tris-HCl, pH 7.4, 150 mM NaCl, 1% NP-40, 0.5% sodium deoxycholate, 0.1% SDS, and 10% glycerol) supplemented with protease inhibitors (Roche) and phospho-protease inhibitors (Santa Cruz). Quantities of proteins were determined by bicinchoninic acid assay (Pierce). Antimouse antibodies were used against pBTK-Y223, BTK (Cell Signaling), and GAPDH (ThermoFisher Scientific).

RNA Sequencing

Isolated splenic B cells from 3 young (3-month-old) and 3 aged (9-month-old) mice per group (euTCL1, euTCL1/HDAC6KO, HDAC6KO, and wild-type) were lysed in Trizol, and messenger-RNA extraction was performed. Normalized expression data from DESeq2 were log transformed. For each group, top-expressed genes were used to perform further analyses.

RNA-Seq was performed using the NuGen Ovation Encore Complete kit, which generates strand-specific total RNA-seq libraries. Following quality-control screening on the NanoDrop to assess 260/230 and 260/280 ratios, the samples were screened on the Agilent BioAnalyzer RNA Nano Chip to generate an RNA Integrity Number. One hundred ng of DNase-treated RNA was then used to generate double-stranded cDNA, which was initiated with selective random priming, allowing for the sequencing of total RNA and avoidance of ribosomal RNA transcripts. Complementary DNA was then fragmented to 200 bp with the Covaris M220 sonicator (Covaris, Inc.), followed by purification with Agencourt RNAClean XP beads (Beckman Coulter, Inc.). End repair and ligation were performed according to the manufacturer's protocol, and strand selection was performed followed by 13 cycles of library amplification. Final libraries were bead-purified and screened for library fragment size distribution using an Agilent BioAnalyzer DNA 1000 Chip (Agilent Technologies). Libraries were quantitated using the Kapa Library Quantification Kit (Roche Sequencing), and were sequenced on one quarter of an Illumina NextSeq 500 150-cycle high-output flow cell in order to generate 35 to 40 million pairs of 75-base reads (Illumina, Inc.).

Reverse transcription and polymerase chain reaction

Total RNA was isolated using Trizol reagent (Invitrogen). Complementary DNA was synthesized from RNA using iScript Reverse Transcriptase (BioRad). Primers against mouse SYK and mouse 18s (Qiagen) were used together with iScript Reaction Mix (BioRad).

Reagents and Antibodies

ACY738 was supplied by Acetylon Pharmaceuticals. All other inhibitors used in experiments were commercially obtained. All inhibitors used for *in vitro* assays were dissolved in dimethyl sulfoxide and stored as 20 mM stock at -20°C.

For murine studies, ACY738 was incorporated into chow at 25 mg/kg and administered to mice orally. Ibrutinib was dissolved in drinking water with 10% cyclodextrin at a final concentration of 15 mg/kg per day per mouse and administered orally, in accordance with a previously established protocol.³

For immunophenotyping analysis of murine CLL, DAPI (4',6-diamino-2-phenylindole, dihydrochloride) exclusion was used for viability staining. Antimouse antibodies were used against CD3 BV786, CD19 Alexa Fluor 700, CD5 PerCP, immunoglobulin M PE, CD4 Pacific Blue, CD8 FITC, CD69 BUV737 (BD Biosciences), and B220 Alexa Fluor 488 (Biolegend). Absolute cell counts were determined using Accucheck counting beads (ThermoFisher Scientific), following the manufacturer's protocol.

For phospho-flow analysis, antibodies were used against pBTK-Y223, pAKT-S473, pERK-T202/Y204 (BD Biosciences), and pSyk-Y525/526 (Cell Signaling), conjugated to Alexa Fluor 647. Phospho-IKK α/β -S176/180 (Cell Signaling) was used with antirabbit secondary antibodies conjugated to Alexa Fluor 647.

For assessment of HDAC6 expression in CLL patient samples, antibodies were used against HDAC6 Alexa Fluor 488 (Novus Biologicals), acetylated alpha-tubulin PE (Cell Signaling), CD19 Alexa Fluor 647, and CD5 PerCP (BD Biosciences). Frozen aliquots of CLL peripheral blood mononuclear cells were thawed and allowed

to recover at 37°C in RPMI media with 50% fetal bovine serum for 1 hour. Samples were fixed using nuclear transcription factor staining buffer set (BD Biosciences) in accordance with the manufacturer's protocol. Cells were stained in the presence of human Fc block (BD Biosciences).

For apoptosis assays, cells were stained with Annexin V BV605 (BD Biosciences) and Live Dead Near Infrared (ThermoFisher Scientific) in the presence of annexin V staining buffer, in accordance with the manufacturer's protocol.

Table S1. Summary of CLL patient characteristics

Patient ID	Gender	Age at Diagnosis	Cytogenetics (FISH)	CD38 Expression >7%	ZAP70 Expression >10%	IgVH Status	Relapsed
CLL1	Female	47	trisomy 12	-	-	Unmutated	Yes
CLL2	Female	50	normal	-	-	Mutated	No
CLL3	Female	71	del 13q, del 17p	+	+	Mutated	No
CLL4	Male	51	trisomy 12	-	-	Mutated	Yes
CLL5	Male	62	del 13q	-	Unknown	Mutated	No
CLL6	Female	59	trisomy 12	Unknown	+	Unknown	Yes
CLL7	Male	58	del 11q, del 13q	+	+	Unmutated	Yes
CLL8	Male	39	del 11q	+	Unknown	Mutated	Yes
CLL9	Male	61	del 13q	-	-	Mutated	No
CLL10	Female	62	normal	-	-	Mutated	No
CLL11	Female	55	trisomy 12	-	Unknown	Unmutated	Yes
CLL12	Male	57	del 13q	+	-	Mutated	No
CLL13	Male	46	del 11q, del 13q	-	-	Unmutated	No
CLL14	Male	56	del 13q	+	+	Mutated	No
CLL15	Male	69	del 11q, del 13q	Unknown	Unknown	Mutated	No
CLL16	Male	58	del 13q	+	-	Unknown	No
CLL17	Male	61	del 13q	-	-	Mutated	No
CLL18	Female	49	del 13q, del 17p, del 12	-	-	Unknown	Yes
CLL19	Male	65	homozygous 13q	+	-	Unmutated	No
CLL20	Female	56	normal	-	-	Unmutated	No
CLL21	Male	46	del 11q	-	-	Unknown	No
CLL22	Female	39	trisomy 12	+	-	Mutated	No
CLL23	Male	64	trisomy 12	+	-	Mutated	No
CLL24	Male	53	normal	+	+	Mutated	No
CLL25	Male	77	del 13q, del 17p	-	-	Mutated	No
CLL26	Female	74	trisomy 12	-	-	Mutated	No
CLL27	Male	49	IgH rearrangement	-	-	Unknown	No
CLL28	Female	49	del 11q, del 13q	+	-	Mutated	No
CLL29	Female	46	del 13q	Unknown	-	Mutated	No
CLL30	Male	61	del 11q, del 13q	-	-	Mutated	No
CLL31	Female	60	del 13q	-	-	Unmutated	No
CLL32	Male	65	normal	+	-	Unknown	No
CLL33	Female	76	normal	-	+	Unmutated	No
CLL34	Female	49	del 11q, IgH rearrangement	+	Unknown	Unmutated	No
CLL35	Male	52	normal	Unknown	Unknown	Unmutated	Yes
CLL36	Female	55	del 13q	+	-	Mutated	No
CLL37	Male	56	del 13q	-	Unknown	Mutated	No
CLL38	Female	57	del 11q, del 13q	+	-	Unmutated	No

Table S2. Gene ontology analysis for disease-related genes uniquely regulated in euTCL1/HDAC6KO mice: top 50 pathways

Enrichment analysis report							
Enrichment by Pathway Maps							
#	Maps	Total	pValue	Min FDR	p-value	FDR	In Data
					TCL1KO_Young-vs.Old_05_Venn_Group_D_GeneList.csv_geneList		
					Network Objects from Active Data		
1	Immune response: Antigen presentation by MHC class I: cross-present	99	2.478E-06	1.340E-03	2.478E-06	1.340E-03	10
2	Signal transduction: Activation of PKC via G-Protein coupled receptor	52	1.304E-04	3.528E-02	1.304E-04	3.528E-02	6
3	Translation: Regulation of EIF2 activity	39	2.933E-04	5.290E-02	2.933E-04	5.290E-02	5
4	Dysregulation of germinal center response in SLE	65	4.497E-04	6.082E-02	4.497E-04	6.082E-02	6
5	Ca(2+)-dependent NF-AT signaling in cardiac hypertrophy	57	1.712E-03	1.664E-01	1.712E-03	1.664E-01	5
6	Immune response: Antigen presentation by MHC class II	118	2.152E-03	1.664E-01	2.152E-03	1.664E-01	7
7	Development: Thyrotrobin signaling	60	2.153E-03	1.664E-01	2.153E-03	1.664E-01	5
8	Development: Negative regulation of STK3/4 (Hippo) pathway and posi	62	2.489E-03	1.683E-01	2.489E-03	1.683E-01	5
9	DNA damage: NHEJ mechanisms of DSBs repair	19	2.820E-03	1.695E-01	2.820E-03	1.695E-01	3
10	Immune response: IL-4-responsive genes in type 2 immunity	70	4.225E-03	2.158E-01	4.225E-03	2.158E-01	5
11	Immune response: IL-3 signaling via ERK and PI3K	102	4.626E-03	2.158E-01	4.626E-03	2.158E-01	6
12	Action of GSK3 beta in bipolar disorder	23	4.930E-03	2.158E-01	4.930E-03	2.158E-01	3
13	CFTR folding and maturation (normal and CF)	24	5.572E-03	2.158E-01	5.572E-03	2.158E-01	3
14	Immune response: Histamine H1 receptor signaling in immune respons	47	5.584E-03	2.158E-01	5.584E-03	2.158E-01	4
15	Immune response: IL-5 signaling via PI3K, MAPK and NF-kB	76	5.996E-03	2.163E-01	5.996E-03	2.163E-01	5
16	Signal transduction: IP3 signaling	49	6.480E-03	2.191E-01	6.480E-03	2.191E-01	4
17	Neurophysiological process: GABA-A receptor life cycle	27	7.788E-03	2.479E-01	7.788E-03	2.479E-01	3
18	Immune response: Innate immune response to RNA viral infection	28	8.627E-03	2.593E-01	8.627E-03	2.593E-01	3
19	Proteolysis: Putative SUMO-1 pathway	29	9.516E-03	2.710E-01	9.516E-03	2.710E-01	3
20	Development: Cytokine-mediated regulation of megakaryopoiesis	57	1.100E-02	2.976E-01	1.100E-02	2.976E-01	4
21	Immune response: TREM1 signaling pathway	60	1.311E-02	3.198E-01	1.311E-02	3.198E-01	4
22	Oxidative stress: Role of Sirtuin1 and PGC1-alpha in activation of antio	60	1.311E-02	3.198E-01	1.311E-02	3.198E-01	4
23	H2AX and Ku70	33	1.359E-02	3.198E-01	1.359E-02	3.198E-01	3
24	Regulation of CFTR activity (normal and CF)	62	1.466E-02	3.236E-01	1.466E-02	3.236E-01	4
25	Transcription: HIF-1 targets	95	1.495E-02	3.236E-01	1.495E-02	3.236E-01	5
26	DNA damage: Role of NFB1 in DNA damage response	13	1.616E-02	3.325E-01	1.616E-02	3.325E-01	2
27	Role of Tissue factor-induced Thrombin signaling in cancerogenesis	65	1.718E-02	3.325E-01	1.718E-02	3.325E-01	4
28	Influence of low doses of Arsenite on Glucose stimulated insulin secre	36	1.721E-02	3.325E-01	1.721E-02	3.325E-01	3
29	Development: Gastrin in differentiation of the gastric mucosa	38	1.989E-02	3.409E-01	1.989E-02	3.409E-01	3
30	Immune response: Gastrin in inflammatory response	69	2.094E-02	3.409E-01	2.094E-02	3.409E-01	4
31	Regulation of degradation of deltaF508-CFTR in CF	39	2.131E-02	3.409E-01	2.131E-02	3.409E-01	3
32	Immune response: Th1 and Th2 cell differentiation	40	2.279E-02	3.409E-01	2.279E-02	3.409E-01	3
33	Intercellular relations in asthma (general schema)	16	2.413E-02	3.409E-01	2.413E-02	3.409E-01	2
34	Translation: (L)-selenoaminoacids incorporation in proteins during tran	41	2.432E-02	3.409E-01	2.432E-02	3.409E-01	3
35	Apoptosis and survival: BAD phosphorylation	42	2.591E-02	3.409E-01	2.591E-02	3.409E-01	3
36	Development: VEGF signaling and activation	42	2.591E-02	3.409E-01	2.591E-02	3.409E-01	3
37	Immune response: PIP3 signaling in B lymphocytes	42	2.591E-02	3.409E-01	2.591E-02	3.409E-01	3
38	Transcription: Transcription factor Tubby signaling pathways	17	2.707E-02	3.409E-01	2.707E-02	3.409E-01	2
39	DeltaF508-CFTR traffic / ER-to-Golgi in CF	17	2.707E-02	3.409E-01	2.707E-02	3.409E-01	2
40	wCFTR traffic / ER-to-Golgi (normal)	17	2.707E-02	3.409E-01	2.707E-02	3.409E-01	2
41	Immune response: CRTH2 signaling in Th2 cells	44	2.924E-02	3.409E-01	2.924E-02	3.409E-01	3
42	Apoptosis and survival: NGF/ TrkA PI3K-mediated signaling	77	2.988E-02	3.409E-01	2.988E-02	3.409E-01	4
43	Immune response: CCR3 signaling in eosinophils	77	2.988E-02	3.409E-01	2.988E-02	3.409E-01	4
44	Neurophysiological process: Glutamic acid regulation of Dopamine D1	45	3.098E-02	3.409E-01	3.098E-02	3.409E-01	3
45	Cell adhesion: Histamine H1 receptor signaling in the interruption of ce	45	3.098E-02	3.409E-01	3.098E-02	3.409E-01	3
46	Immune response: PGE2 signaling in immune response	45	3.098E-02	3.409E-01	3.098E-02	3.409E-01	3
47	Development: Activation of ERK by Alpha-1 adrenergic receptors	45	3.098E-02	3.409E-01	3.098E-02	3.409E-01	3
48	High shear stress-induced platelet activation	46	3.279E-02	3.409E-01	3.279E-02	3.409E-01	3
49	Immune response: Naive CD4+ T cell differentiation	46	3.279E-02	3.409E-01	3.279E-02	3.409E-01	3
50	Development: GDNF family signaling	46	3.279E-02	3.409E-01	3.279E-02	3.409E-01	3

Figure S1. Flow cytometry analysis of CLL patient and normal peripheral blood mononuclear cells (PBMCs). Cells of interest were gated on singlets using forward scatter height vs. forward scatter area parameters and nonviable cells (Live Dead Yellow-positive) were excluded. Median fluorescence intensity of HDAC6 was determined for the CD19+ CD5+ (CLL B cells) population. All markers were gated according to fluorescence-minus-one or isotype controls. HDAC6 fluorescence-minus-one control is indicated as grey histogram. Red arrows denote the order of gating strategy. (A) Representative of CLL patient cells analysis. (B) Representative of normal donor cells analysis. Abbreviations: CLL, chronic lymphocytic leukemia; PMBC, peripheral blood mononuclear cells.

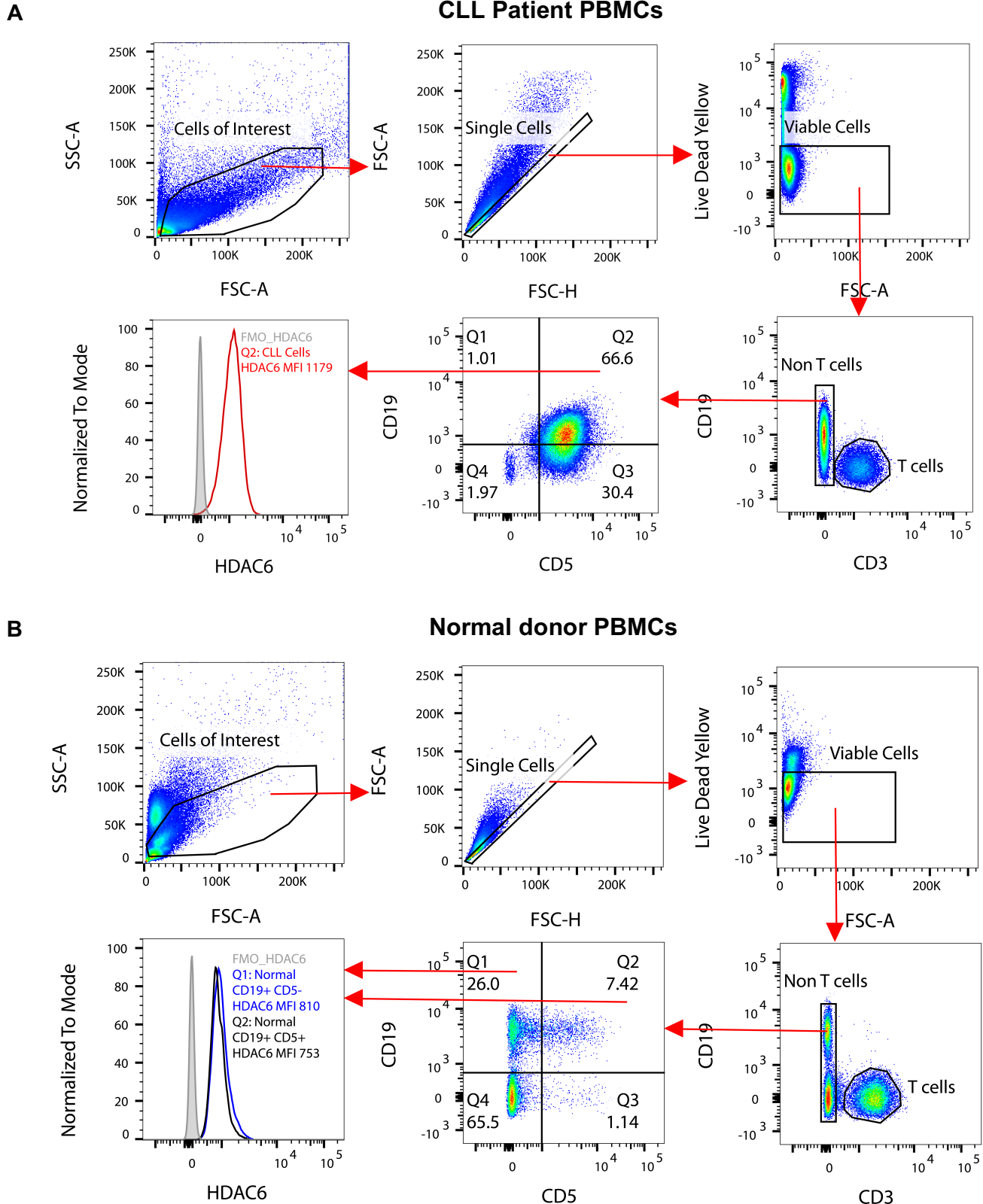


Figure S2. Analysis of HDAC6-deficient CLL mouse model. (A) Western blot showing expression of HDAC6 protein in WT, euTCL1, HDAC6KO or euTCL1/HDAC6KO murine B cells. (B) Flow cytometry showing expression of HDAC6 protein in WT, euTCL1, HDAC6KO or euTCL1/HDAC6KO murine B cells. (C) Flow cytometry analysis showing TCL1 protein expression is similar in euTCL1 B cells and euTCL1/HDAC6KO B cells. (D) Flow cytometry analysis showing functional inhibition of HDAC6 in euTCL1/HDAC6KO B cells demonstrated by increased acetylation of alpha-tubulin, a cytoplasmic substrate of HDAC6, than in the WT cohort. Abbreviations: CLL, chronic lymphocytic leukemia; WT, wild-type mouse.

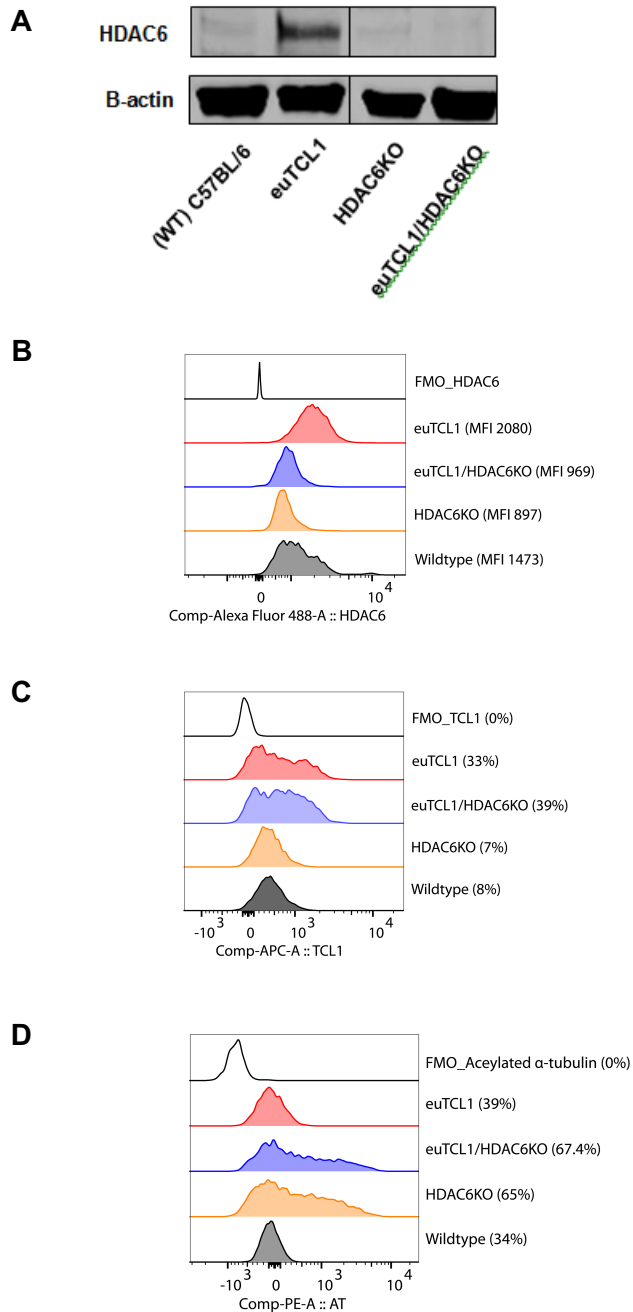


Figure S3. Quantification of tumor burden in CLL mice. Flow cytometry analysis of tumor burden in splenocytes of (A) euTCL1 and (B) euTCL1/HDAC6KO mice. Cells of interest were gated on singlets using forward scatter height vs. forward scatter area parameters, and nonviable cells (4',6-Diamidino-2-Phenylindole, Dihydrochloride -positive) were excluded. The CD3- CD19+ B220+ CD5- were gated as normal B cells and CD3- CD19+ B220+ CD5+ were gated as malignant CLL B cells. CD5 fluorescence-minus-one control is displayed as grey dots. Red arrows denote the order of gating strategy.

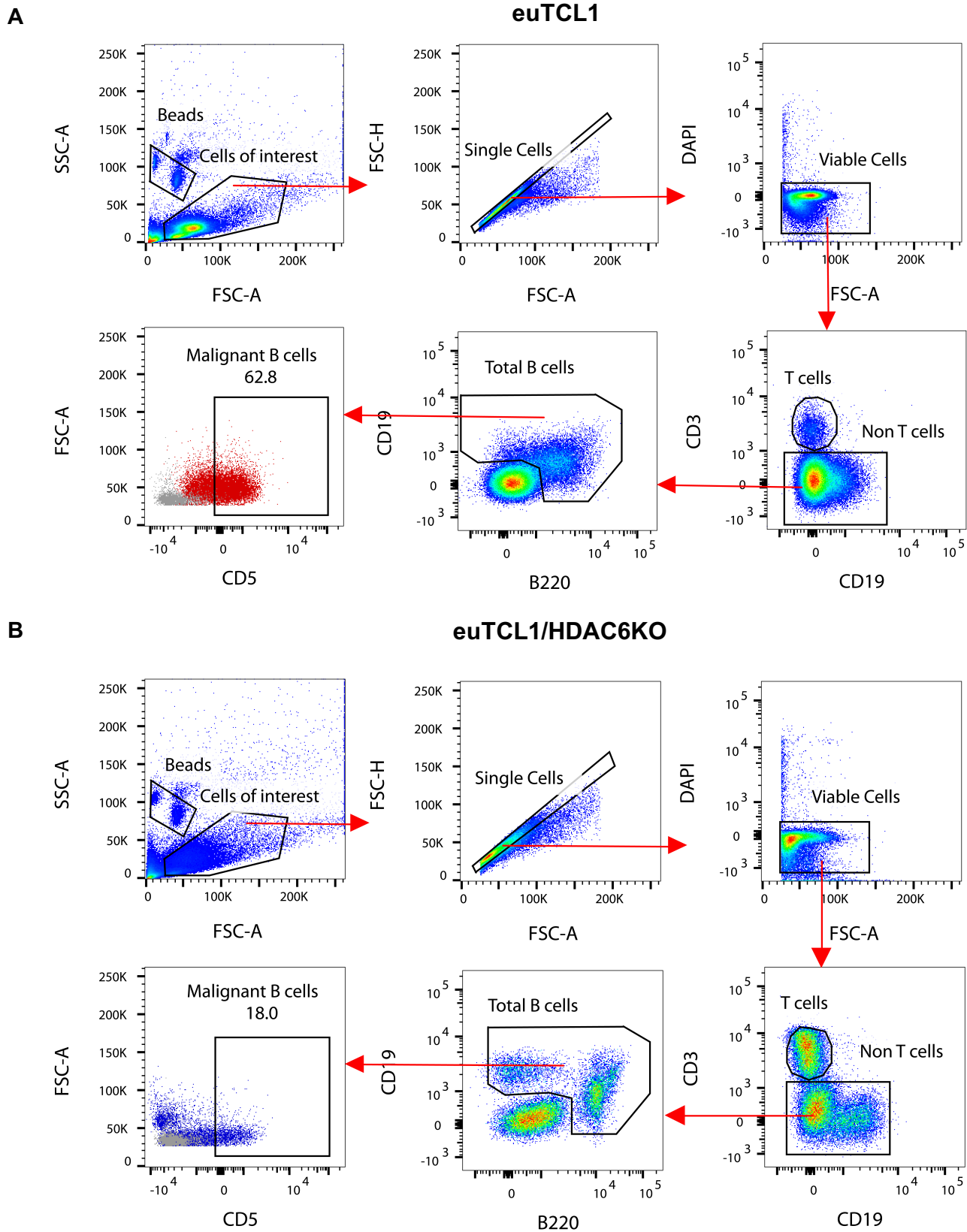


Figure S4. Hierarchical clustering of top 50 differentially expressed genes, showing similarities in gene expression patterns among mice used in RNA-sequencing analyses. (A) Young group. (B) Old group.

A

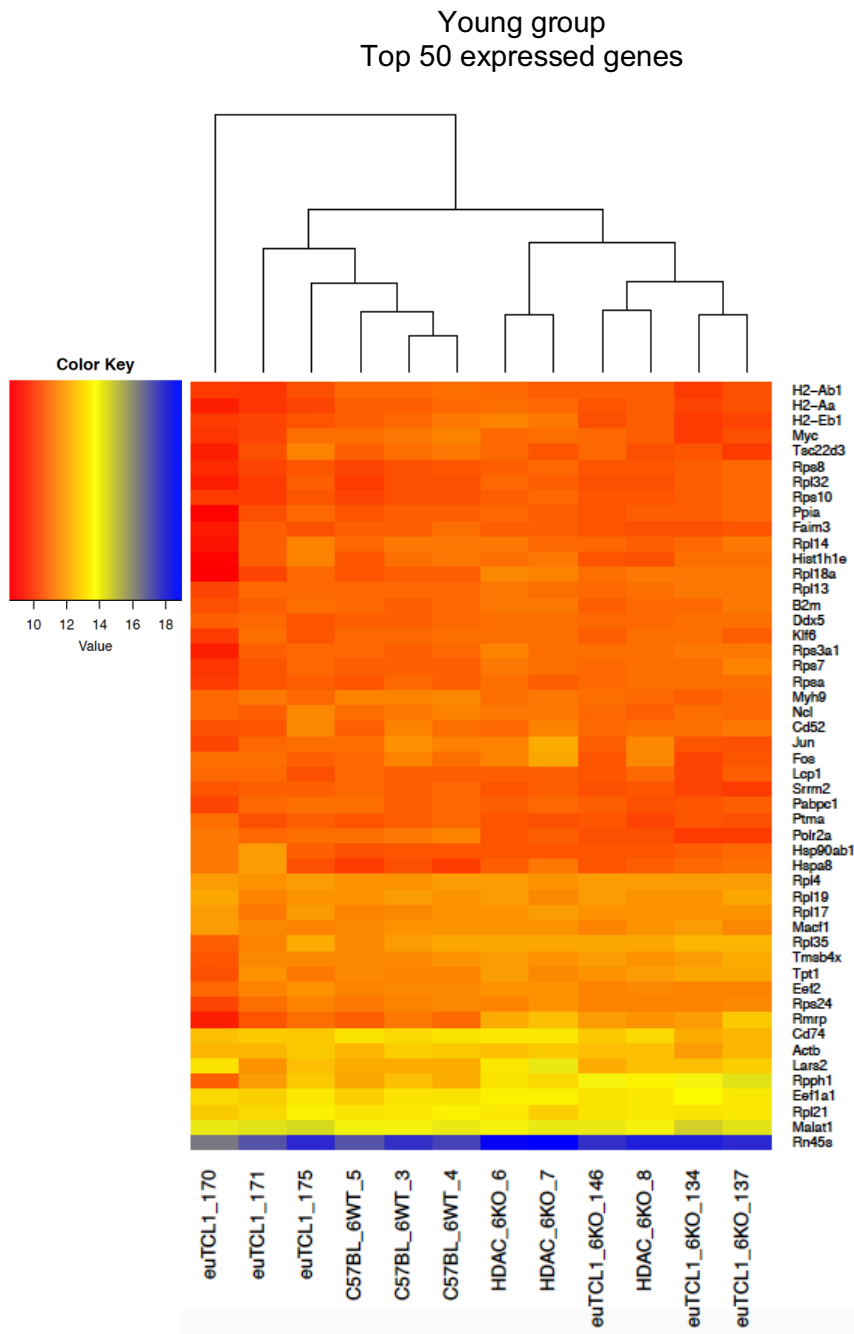


Figure S4/Continued

B

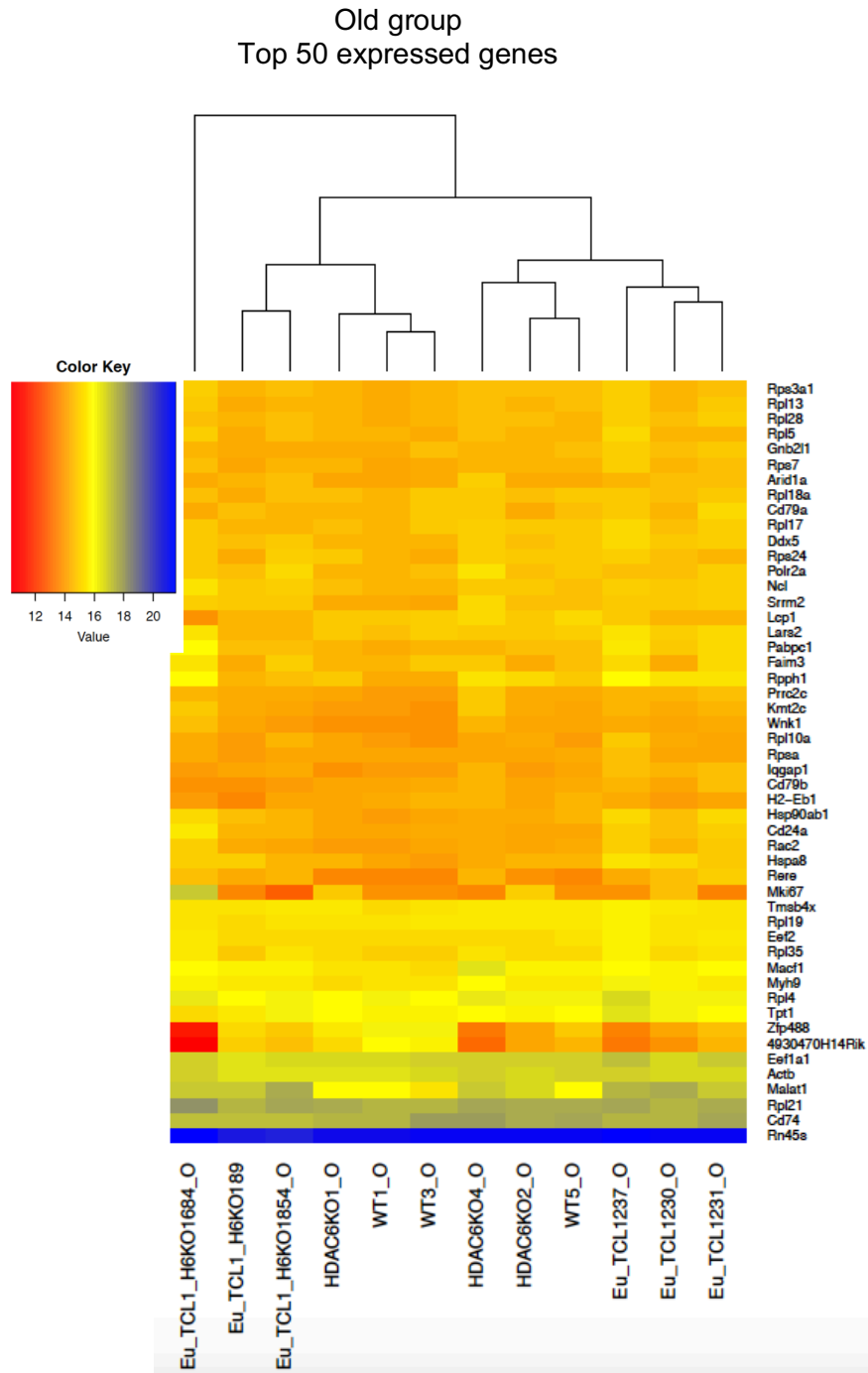
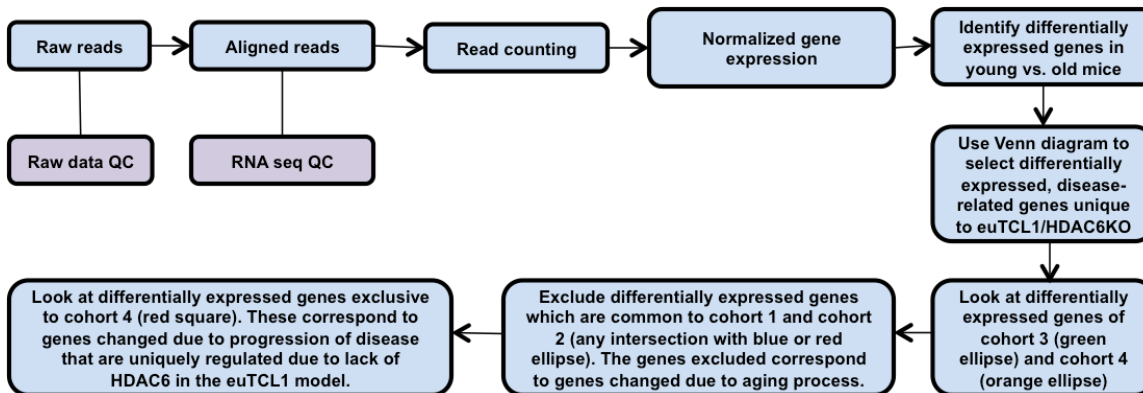


Figure S5. RNA-sequencing analysis of young and old mice. (A) Table showing cohorts of mice used for analysis and types of genes identified by each. (B) Flow chart describing step-by-step analysis process used to identify genes of interest (C) Venn diagram displaying the number of differentially expressed genes either exclusive to or common to each cohort. Venn diagram was used in the identification of genes of interest. (D) Western blot showing expression of SYK protein in isolated murine B cells (from spleens) along with graphed densitometry of bands (n = 3 mice per group).

A

Cohort 1. young WT vs. old WT	Identify differentially expressed genes due to aging only
Cohort 2. young HDAC6KO vs. old HDAC6KO	Identify differentially expressed genes due to aging only that are affected by lack of HDAC6
Cohort 3. young euTCL1 vs. old euTCL1	Identify differentially expressed genes due to both aging and disease
Cohort 4. young euTCL1/HDAC6KO vs. old euTCL1/HDAC6KO	Identify differentially expressed genes due to both aging and disease that are affected by lack of HDAC6

B



C

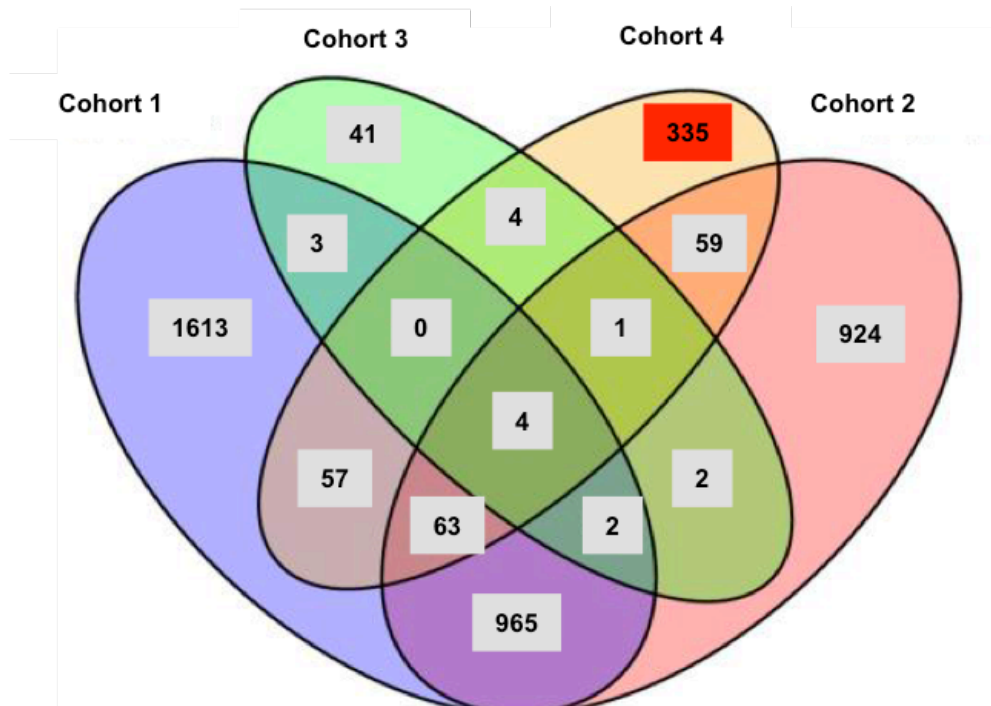


Figure S5/Continued

D

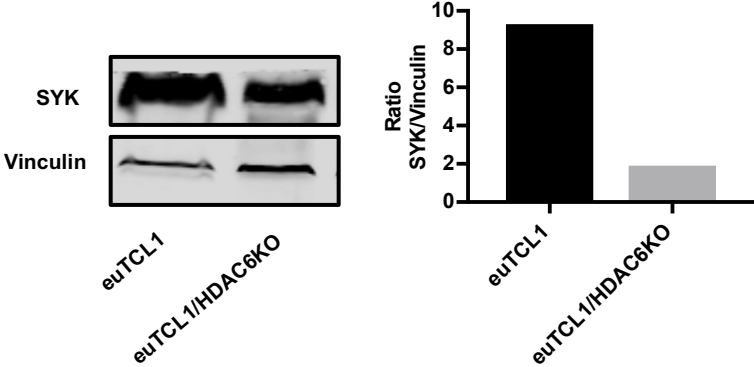


Figure S6. HDAC6-selective range of ACY738 in CLL cell lines. (A) OSU-CLL and Mec2 were treated with ACY738 in increasing concentrations for 24 hours, and flow cytometry analysis was performed to detect acetylation status of alpha-tubulin and histone 3 in viable cells. Increased acetylation of alpha-tubulin compared to histone 3 indicated selectivity for HDAC6 inhibition (B) Heat map showing biochemical potency of ACY738 for HDAC1-9 compared to pan-HDAC inhibitor panobinostat and another HDAC6 selective inhibitor, ACY1215. (C) Growth kinetics of Mec2 in culture with ACY738 at 1 μ M or vehicle for indicated period. (D) Cell cycle analysis in Mec2 determined by Ki67/7AAD staining after 24 hours of indicated treatments. (E) Apoptosis analysis in Mec2 determined by Annexin V/viable staining following treatment of Mec2 with ACY738 for 24 hours. (F) Phosphorylation of indicated molecules was measured following stimulation with 10 μ g/mL antihuman immunoglobulin M in Mec2. (G) Expression of intracellular MCL1 and BCL-2 protein analyzed by flow cytometry, after incubating Mec2 with indicated concentrations of ACY738.

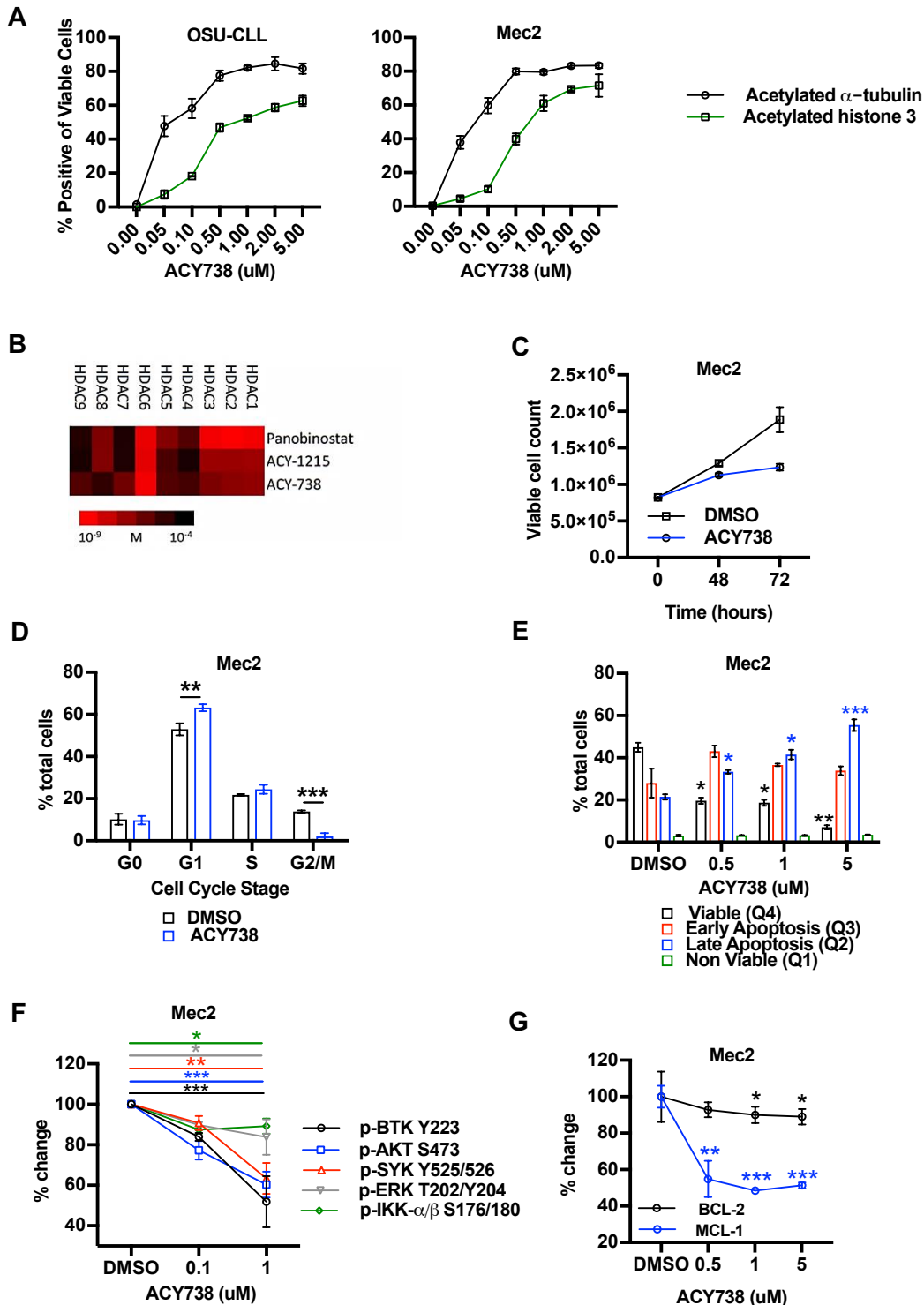
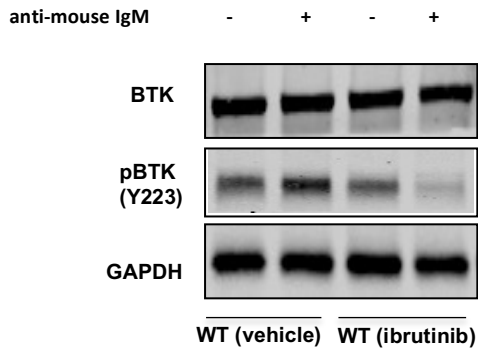


Figure S7. Functional activity of ibrutinib drinking water. Western blot showing activity of ibrutinib delivered via drinking water. WT mice (n = 3 per group) were supplied with ibrutinib drinking water or regular drinking water (vehicle) for 3 days. Mice were sacrificed, and total B cells were isolated by magnetic separation from homogenized splenocytes. Phosphorylation of BTK at Y223 was measured following 30 minutes of stimulation with plate-bound antimouse IgM (10 μ g/mL). Abbreviations: GAPDH, glyceraldehyde 3-phosphate dehydrogenase; IgM, immunoglobulin M; pBTK, phosphorylated Bruton's tyrosine kinase; WT, wild-type mouse.



REFERENCES

1. Hallek M, Cheson BD, Catovsky D, et al. Guidelines for diagnosis, indications for treatment, response assessment and supportive management of chronic lymphocytic leukemia. *Blood*. 2018.
2. Chou TC. Drug combination studies and their synergy quantification using the Chou-Talalay method. *Cancer Res*. 2010;70(2):440-446.
3. Woyach JA, Bojnik E, Ruppert AS, et al. Bruton's tyrosine kinase (BTK) function is important to the development and expansion of chronic lymphocytic leukemia (CLL). *Blood*. 2014;123(8):1207-1213.